JOURNAL OF GEOPHYSICAL RESEARCH: OCEANS, VOL. 118, 1–8, doi:10.1002/jgrc.20182, 2013

Relationships between inherent optical properties and the depth of penetration of solar radiation in optically complex coastal waters

Alex Cunningham,[1] Leanne Ramage,[1] and David McKee[1]

Received 23 January 2013; revised 25 March 2013; accepted 25 March 2013.

[1] The attenuation of downward planar irradiance can be quantified by $\overline{K}_d(E_{10\%}, \lambda)$, the diffuse attenuation coefficient calculated from the surface to the depth where the irradiance E_d at wavelength λ falls to 10% of its surface value. Theoretical studies by Gordon (1989) and Lee et al. (2005a) suggest that $\overline{K}_d(E_{10\%}, \lambda)$can be derived from the absorption coefficient, $a(\lambda)$ and the backscattering coefficient, $b_b(\lambda)$, using equations incorporating either the solar zenith angle (θ_a) or the subsurface distribution function (D_0) and empirical coefficients derived by radiative transfer modeling. These results have not, however, been validated against in situ measurements. We have therefore assessed the performance of both models using measurements of $a(\lambda)$, $b_b(\lambda)$, and $\overline{K}_d(E_{10\%}, \lambda)$ for 100 stations in UK coastal waters. Best results were obtained from the Lee et al. (2005a) model, for which over 90% of the predicted $\overline{K}_d(E_{10\%}, \lambda)$ values in the 440 nm to 665 nm range were within ± 0.1 m^{-1} of those measured in situ. A strong linear relationship ($R^2 > 0.95$, mean relative difference 5.4%) was found between $\overline{K}_d(E_{10\%})$ at 490 nm and the reciprocal of the depth of the midpoint of the euphotic zone ($z_{10\%}$, PAR). This allowed ($z_{10\%}$, PAR) to be predicted from measured values of a(490 nm), b_b(490 nm) and θ_a, using the Lee et al. model as an intermediate step, with an RMS error of 1.25 m over the 2.5–25.0 m range covered by our data set.

Citation: Cunningham, A., L. Ramage, and D. McKee (2013), Relationships between inherent optical properties and the depth of penetration of solar radiation in optically complex coastal waters, *J. Geophys. Res. Oceans*, *118*, doi:10.1002/jgrc.20182.

1. Introduction

[2] Variations in the depth of penetration of solar radiation play an important role in the physics and biology of coastal water columns. Examples include the solar heating of surface layers [*Zaneveld et al*., 1981; *Kirk*, 1988; *Rochford et al*., 2001], control of the depth to which net phytoplankton production can be sustained [*Behrenfeld and Falkowski*, 1997], the effectiveness of visual prey detection [*Aksnes and Giske*, 1993], and the degree of illumination of benthic communities [*Gattuso et al*., 2006]. These phenomena have traditionally been studied in isolation, but recent work indicates that there are strong interactions between changes in water transparency, thermal effects, biological production, and biogeochemical cycling [*Cahill et al*., 2008; *Zhai et al*., 2011]. Solar illumination at the sea surface is conventionally measured as spectrally resolved downward planar irradiance, $E_d(\lambda)$, and the attenuation of this quantity with depth (z) can be described [*Mobley*, 1994] by the diffuse attenuation coefficient $K_d(z,\lambda)$, defined as

$$K_d(z,\lambda) = -\frac{d(\ln E_d(z,\lambda))}{dz} = -\frac{1}{E_d(z,\lambda)} \lim_{\Delta z \to 0} \frac{\Delta E_d(z,\lambda)}{\Delta z}. \quad (1)$$

[3] Consequently, in order to determine values of $K_d(z,\lambda)$ in situ, $E_d(z, \lambda)$ should be measured at depths which are sufficiently closely spaced that a further reduction in Δz would have no significant effect on the calculated $K_d(z,\lambda)$ value. However practical limitations, including the finite data acquisition rate of profiling radiometers and the relatively wide spacing of instruments on moored arrays, mean that $E_d(z,\lambda)$ is often measured over intervals that are wider than those required to satisfy equation (1). This makes it necessary to introduce a slightly different quantity, $\overline{K}_d(z_1 \to z_2, \lambda)$, which describes the attenuation of downward planar irradiance over a finite interval

$$\overline{K}_d(z_1 \to z_2, \lambda) = \frac{\ln E_d(z_1,\lambda) - \ln E_d(z_2,\lambda)}{(z_2 - z_1)}. \quad (2)$$

[4] *Lee et al*. [2005a] introduced the notation $\overline{K}_d(E_{10\%}, \lambda)$ for the case where $\overline{K}_d(z_1 \to z_2, \lambda)$is calculated from immediately beneath the surface to the depth where $E_d(\lambda)$ falls to 10% of its surface value. Since $K_d(z,\lambda)$ is an apparent optical property (*AOP*) which

[1]Physics Department, University of Strathclyde, Glasgow, UK.

Corresponding author: A. Cunningham, Physics Department, University of Strathclyde, 107 Rottenrow, Glasgow G4 0NG, UK. (a.cunningham@strath.ac.uk)

2169-9275/13/10.1002/jgrc.20182

depends not only on the inherent optical properties (*IOPs*) of the water column, but also on the angular structure of the light field which changes with depth, $\overline{K}_d(E_{10\%}, \lambda)$ is not necessarily equal to the average value of $K_d(z, \lambda)$ over the same depth interval [*Gordon*, 1989]. Early attempts to derive approximate relationships between $\overline{K}_d(z_1 \rightarrow z_2, \lambda)$ and *IOPs* employed expressions involving the coefficients of absorption, $a(\lambda)$, and scattering, $b(\lambda)$ [*Gordon et al*., 1975; *Kirk*, 1984], but the use of the backscattering coefficient (b_b) rather than the total scattering coefficient (b) would permit a more direct link to remote sensing observations. Two slightly different approaches to this problem have been published by *Gordon* [1989] and *Lee et al*. [2005a]. Both are based on the statistical fitting of empirical expressions to extensive radiative transfer calculations, and their validity depends on the extent to which the assumptions incorporated in these calculations are representative of real water columns.

[5] The *Gordon* [1989] model can be written as

$$\overline{K}_d(E_{10\%}, \lambda) = D_0\Big[k_1(a(\lambda)+b_b(\lambda)) + k_2(a(\lambda)+b_b(\lambda))^2 + k_3(a(\lambda)+b_b(\lambda))^3\Big], \quad (3)$$

where D_0 is the distribution function for downward irradiance just below the sea surface. D_0 varies from 1.02 to 1.35 depending on wavelength, solar angle and cloud cover, with solar angle being the most important determining factor. The constants k_1, k_2, and k_3 in equation (3) have values of 1.3197, −0.7559, and 0.4655 respectively. The model proposed by *Lee et al*. [2005a] employs a two-flow formulation of the radiative transfer problem to partially separate the contributions of $a(\lambda)$ and $b_b(\lambda)$, resulting in the expression

$$\overline{K}_d(E_{10\%}, \lambda) = (1+0.005\theta_a)a(\lambda) + 4.18\Big(1-0.52e^{-10.8a(\lambda)}\Big)b_b(\lambda), \quad (4)$$

where θ_a is the solar zenith angle. In a subsequent paper, *Lee et al*. [2005b] derived $\overline{K}_d(E_{10\%}, \lambda)$ from remote sensing reflectance (R_{rs}) in two stages by (i) estimating the coefficients a and b_b from R_{rs} and (ii) using these a and b_b values to estimate $\overline{K}_d(E_{10\%}, \lambda)$. This two-stage procedure performed well in Case 2 waters, providing indirect support for the model proposed by *Lee et al*. [2005a] relating $\overline{K}_d(E_{10\%}, \lambda)$ to a and b_b. To date, however, no independent comparisons of equations (3) and (4) with in situ measurements in optically complex waters have been published. Such comparisons are necessary for validation purposes because radiative transfer calculations inevitably make simplifying assumptions about poorly measured variables such as volume scattering functions, the specific optical properties of individual optically significant constituents, and the distribution of direct and indirect solar irradiances. In this paper, therefore, we compare predictions of $\overline{K}_d(E_{10\%}, \lambda)$ derived from equations (3) and (4) with measurements made in situ in a range of water types located off the west coast of the United Kingdom. The data set assembled for this purpose also made it possible to investigate the relationship between measured values of $\overline{K}_d(E_{10\%}, \lambda)$ and the depth of penetration of spectrally integrated photosynthetically available radiation (*PAR*) in these waters.

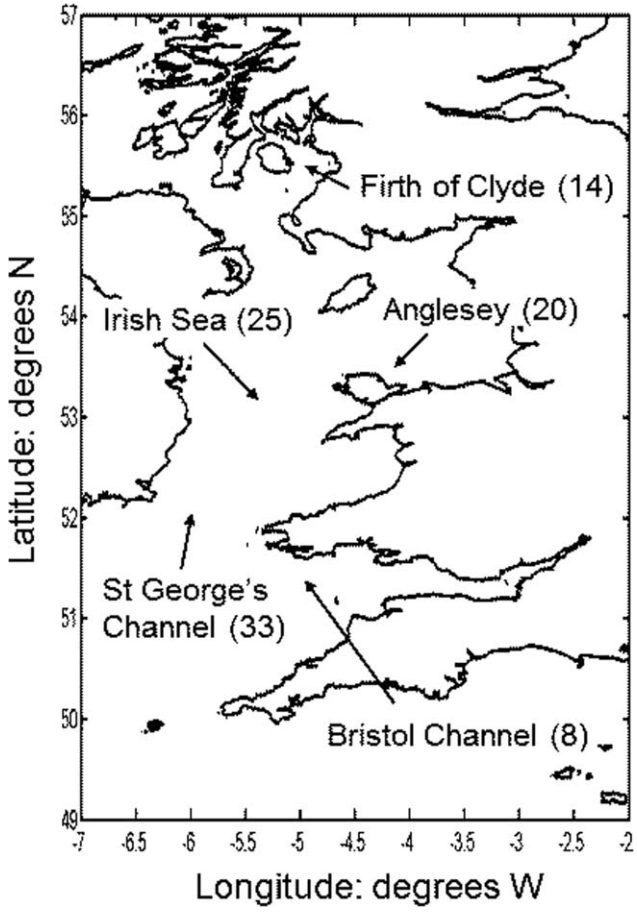

Figure 1. Map of the survey area, with the figures in

2. Methods

[6] The observations used in this paper were made during six cruises carried out in the years 2001–2006. Stations were selected where a complete set of optical and chemical measurements were available, and the attenuation coefficient was approximately constant (to within 10%) over the top 20 m of the water column, with no obvious trend with depth. They covered a wide range of water types including an outer estuary (the Bristol Channel), a semienclosed shelf sea (the Irish Sea) and a system of fjord basins (the Clyde Sea) at the locations indicated in Figure 1. Concentrations of phytoplankton (measured as chlorophyll a), mineral particles and colored dissolved organic matter (measured as the absorption coefficient of dissolved material at 440 nm) were determined by the methods described in *Neil et al*. [2011].

[7] Measurements of downward planar irradiance, $E_d(\lambda)$ were made in 10 nm wavebands centered on 412, 443, 490, 510, 554, 665 and 700 nm using a SeaWiFS Profiling Multichannel Radiometer (Satlantic) and processed to give readings at 1 m depth intervals using ProSoft 7.7. The SPMR was deployed at least 20 m from the ship to avoid

shadow effects and instrument casts were quality controlled for constant solar illumination using a deck sensor. It was difficult to acquire E_d data close to the sea surface due to a combination of wave effects and the problem of holding the instrument in position without introducing a significant degree of tilt from the vertical. Consequently, most SPMR profiles started at a depth of 1 m or 2 m (depending on the sea state), where the tilt angle was less than 10°, and it was necessary to extrapolate them to obtain estimated subsurface irradiance values. This extrapolation was performed by a least-squares fit to log-transformed E_d (λ) data from the top 5 available depths. Values for photosynthetically active radiation (PAR) were calculated by converting SPMR downward irradiance measurements to units of quanta m^{-2} s^{-1} nm^{-1} and carrying out trapezoidal integrations across the visible waveband. Artifacts can arise in deriving K_d values from E_d profiles due to Raman scattering and chlorophyll fluorescence, both of which transfer photons from shorter to longer wavelengths within the water column. However Raman scattering has a negligible effect on K_d in the top few attenuation lengths [*Smith and Marshall*, 1994] and is therefore not a major factor in the present study, while chlorophyll fluorescence is confined to a band centered on 685 nm [*Gower et al*., 1999] which was not measured by the SPMR.

[8] Nonwater absorption and beam attenuation coefficients (a_{nw} and c_{nw}) were measured in nine wavebands of 10 nm full width half maximum, centered on 412, 440, 488, 510, 532, 555, 650, 676, and 715 nm, using a WET Labs ac-9 absorption and attenuation meter which was regularly calibrated against Milli-Q ultra pure water blanks. The ac-9 data were corrected for variations in temperature and salinity using data from a SeaBird SBE 19 CTD deployed in the same instrument cage and the coefficients given in *Sullivan et al*. [2006]. Compensation for the incomplete collection of scattered light in the absorption tube was carried out using the proportional method of *Zaneveld et al*. [1994], and total absorption coefficients (a_t) were derived by adding the pure water values tabulated in *Pope and Fry* [1997] to the corrected a_{nw} data. The use of this correction procedure for ac-9 data has been criticized on the grounds that it assumes zero nonwater absorption at 715 nm [*Tassan and Ferrari*, 2003; *Tzortziou et al*., 2006]. Monte Carlo modeling by *Leymarie et al*. [2010] suggested that this could lead to a_{nw} being under-estimated by up to 5% at 412 nm and 50% at 676 nm in waters where mineral particles were the optically dominant constituent. However their analysis was based on the assumption that the absorption coefficient of nonalgal particles at 750 nm was 25% of its value at 440 nm, which is considerably higher than the 5% suggested by *Tzortziou et al*. [2006]. The significance of these potential errors is minimized in the present study because absorption by suspended particles at most stations makes a relatively small contribution to the total absorption coefficient at the red end of the spectrum. At 676 nm, for example, the pure water absorption coefficient is 0.45 m^{-1} while 75% of the measured nonwater absorption coefficients are less than 0.06 m^{-1}.

[9] Five of the ac-9 wavebands (412 to 554 nm) were sufficiently close to those measured by the SPMR to be regarded as matches for the purpose of modeling diffuse attenuation coefficients. For the SPMR band at 665 nm, the total absorption coefficient was estimated by adding the nonwater absorption coefficient measured at 676 nm to the pure water coefficient at 665 nm. The justification for this approximation was the dominant role played by water absorption at the far red end of the spectrum.

[10] Backscattering coefficients, $b_b(\lambda)$ in two wavebands centered on 470 nm and 676 nm were measured using a HOBI Labs HS-2 backscattering meter. Compensation for absorption and scattering was applied to the HS-2 data using the sigma correction method recommended by the manufacturer, together with a_{nw} and b_{nw} values recorded by the ac-9 during each deployment. Since the HS-2 measured backscattering in only two wavebands, the data were linearly extrapolated to give estimated values for ac-9 wavebands. The values of $a(\lambda)$ and $b_b(\lambda)$ used for the calculations of $\overline{K}_d(E_{10\%}, \lambda)$ in this paper were obtained by averaging instrument readings from the upper 5 m of the water column.

3. Results

[11] The range of concentrations of the main optically significant constituents present in surface water samples is shown for all stations in Figure 2. Chlorophyll a concentrations were generally low (less than 2 mg m^{-3} for 90% of the stations) but blooms in the Firth of Clyde produced values extending up to 14 mg m^{-3}. Suspended mineral particles were below 2 g m^{-3} in the central Irish Sea and St George's Channel, with higher concentrations (up to 12 g m^{-3}) occurring in shallower waters off Anglesey and in the Bristol Channel. Colored dissolved organic matter concentrations, measured as the absorption coefficient of dissolved material at 440 nm, were mostly less than 0.2 m^{-1} but values up to 0.5 m^{-1} were found in the Firth of Clyde. There was no significant correlation between the concentrations of chlorophyll *a* and those of the other materials. The stations sampled therefore fall into the Case 2 optical classification of *Morel and Prieur* [1977], and are fairly representative of moderately turbid coastal waters. The solar zenith angles under which radiometric profiles were collected (Figure 2) were always greater than 30°, and some stations were occupied with the sun within 10° of the horizon. The fractional decrease in downward irradiance spectra with depth for a typical Firth of Clyde station (Figure 3) shows the characteristically rapid loss of red and blue light with depth in these waters. The same data are plotted for individual wavebands on a logarithmic scale in Figure 4, in which the best-fit lines drawn through the data confirm that attenuation for each waveband was close to exponential with depth. The inverse slopes of these lines correspond to the depth averaged attenuation coefficients defined in equation (2). Attenuation is therefore strongly wavelength dependent, being lowest in the green waveband (554 nm) and highest in the far red (700 nm). The vertical lines on the figure indicate logarithm values (−2.3 and −4.6) corresponding to irradiances of 10% and 1% of surface values, and the intersection of these lines with the plotted data allow depths corresponding to these percentages to be read off for each waveband on the *y* axis. The distribution of $\overline{K}_d(E_{10\%}, \lambda)$ measurements in three representative wavebands at 443, 554, and 665 nm (Figure 5) provides confirmation that light in the middle of the visible

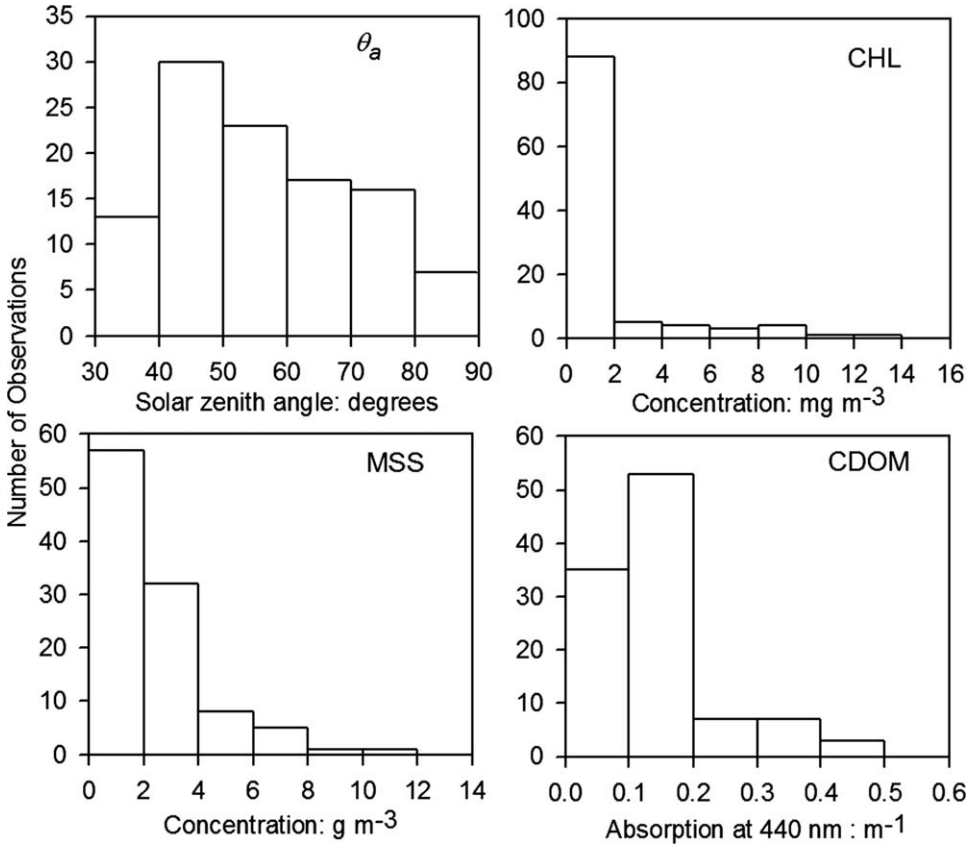

Figure 2. The top left plot shows the distribution of solar zenith angles for all 100 stations. The others show the

spectrum suffered the least attenuation at most of the stations sampled .

[12] Calculations of $\overline{K}_d(E_{10\%}, \lambda)$ using the Gordon model expressed in equation (3) require a value for the distribution function, D_0. The variation of this function with wavelength is less than 2%, but it depends significantly on solar zenith angle. In clear sky conditions it ranges from 1.15 at 40° to 1.35 at 80°. For diffuse solar inputs, which are fairly representative of the cloudy conditions under which most stations were occupied, D_0 assumes an intermediate value of 1.2. The results of least-squares linear regressions between $\overline{K}_d(E_{10\%}, \lambda)$values measured using the SPMR and those predicted by the Gordon model with $D_0 = 1.2$ are summarized in Table 1. If the far red band is excluded (it was not considered in Gordon's original analysis), $\overline{K}_d(E_{10\%}, \lambda)$ values calculated using equation (3) are reasonably well correlated with in situ observations (R^2 lies in the range 0.84–0.87) but are consistently underestimated (slopes, m, are generally around 0.6). It is possible to force the Gordon model to return results that bear a 1:1 relationship to the measured values at 488 nm, while preserving the R^2 performance, by using D_0 values of around 2 (with some dependence on wavelength). However D_0 has a physical meaning (it is the photon distribution function), and setting it to an arbitrary and physically unrealistic value means replacing the analytical element of the Gordon model by an empirical adjustable parameter.

[13] $\overline{K}_d(E_{10\%}, \lambda)$values calculated using the Lee et al. model, equation (4), are plotted against those obtained from SPMR profiles in Figure 6, and regression results are also shown in Table 1. The best-line slopes (m) for wavebands in the range 440–555 nm are close to unity (0.96–0.98) and offsets (c) are very low. The solid lines on the

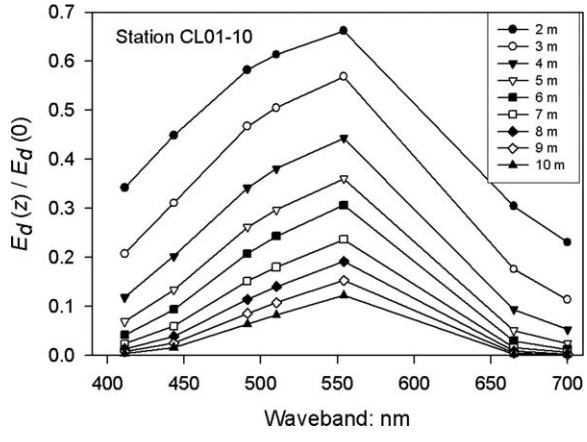

Figure 3. Downward irradiance spectra expressed as a fraction of subsurface values, measured at 1 m intervals in

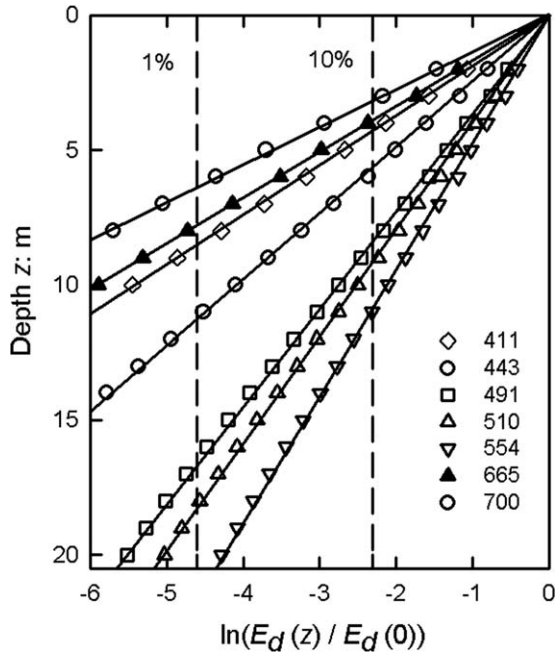

Figure 4. Logarithmic decrease in solar irradiance with depth in a typical coastal water column (Station CL01–10, as in Figure 3.).

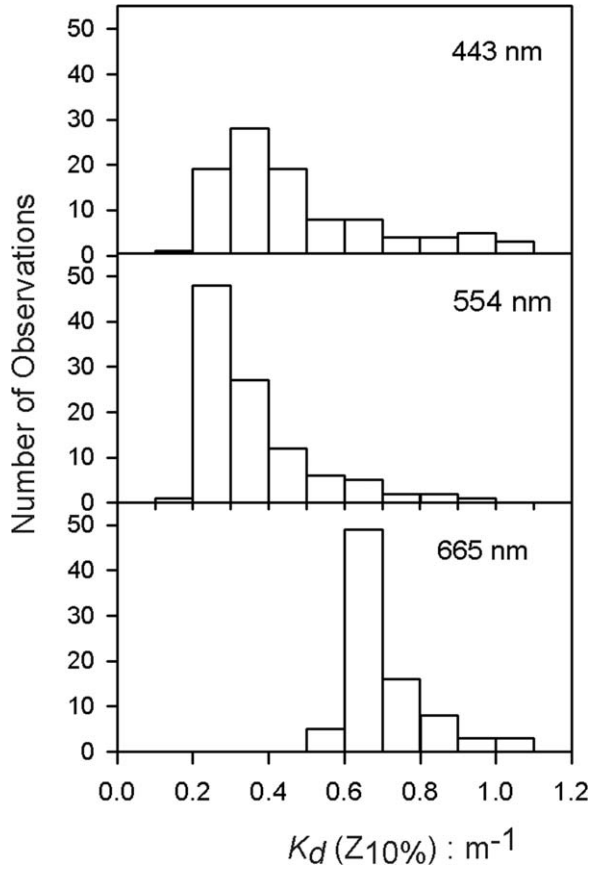

Figure 5. Distribution of attenuation coefficients for

Table 1. Summary of Results for Least-Squares Regressions of $\overline{K}_d(E_{10\%}, \lambda)$ Calculated Using equations (3) and (4) Against In Situ Measurements Using a Profiling Radiometer

λ	m	c	R^2
Equation (3): *Gordon* [1989]			
412	0.65	+0.04	0.85
440	0.76	+0.01	0.87
490	0.63	+0.02	0.85
510	0.60	+0.03	0.84
555	0.52	+0.05	0.85
665	0.38	+0.40	0.69
Equation (4): *Lee et al.* [2005a, 2005b]			
412	0.87	−0.01	0.95
440	0.98	−0.03	0.97
490	0.96	+0.03	0.94
510	0.96	−0.02	0.94
555	0.96	−0.02	0.92
665	0.89	+0.12	0.88

plots in Figure 6 indicate theoretically perfect (1:1) recoveries, and the dotted lines show boundaries for recoveries within $\pm$ 0.1 m^{-1} of the 1:1 lines. For six wavebands (440–665 nm) at least 90% of the data points fall within $\pm$0.1 m^{-1} of the model predictions, but this is reduced to 80% for the 412 nm waveband. We have no definitive explanation for the reduction in the performance of the model at 412 nm, which may be the result of a systematic error in ac-9 or SPMR measurements in this waveband or due to the assumption of linearity in the extrapolation of the backscattering coefficients. The difficulties encountered in obtaining full optical closure between measurements of inherent optical properties and radiometric profiles are well documented in the literature [*Zaneveld*, 1989; *Tzortziou et al*., 2006; *Chang et al*., 2007].

[14] The discrepancy between the Lee et al. and Gordon models appears to originate in their different response to changes in the angular distribution of the underwater light field. Both models explicitly incorporate a parameter for solar zenith angle, and so the discrepancy arises mainly from the degree to which the solar beam is diffused by scattering in the water column. We have carried out exploratory calculations which indicate that the two models give similar results for low (oceanic) backscattering coefficients, but that the Gordon model significantly under-estimates K_d as the backscattering coefficient increases to the values which are typical of coastal waters. Thus, the Gordon model works well for the conditions under which it was derived, but copes less well than the Lee et al. model with the range of backscattering coefficients that may be encountered in shelf seas.

[15] Studies of primary productivity often assume that the attenuation of PAR with depth can be represented by a single exponential term, which leads to the introduction of the quantity K_d (PAR) by analogy with equation (1). This can give rise to theoretical difficulties, since PAR is an integral made up of components which are attenuated at different rates with depth (see Figure 4). However the depths at which PAR falls to 1% and 10% of its subsurface value ($z_{1\%}$,PAR; $z_{10\%}$,PAR) can be defined with no ambiguity, and these are conventionally taken to represent the

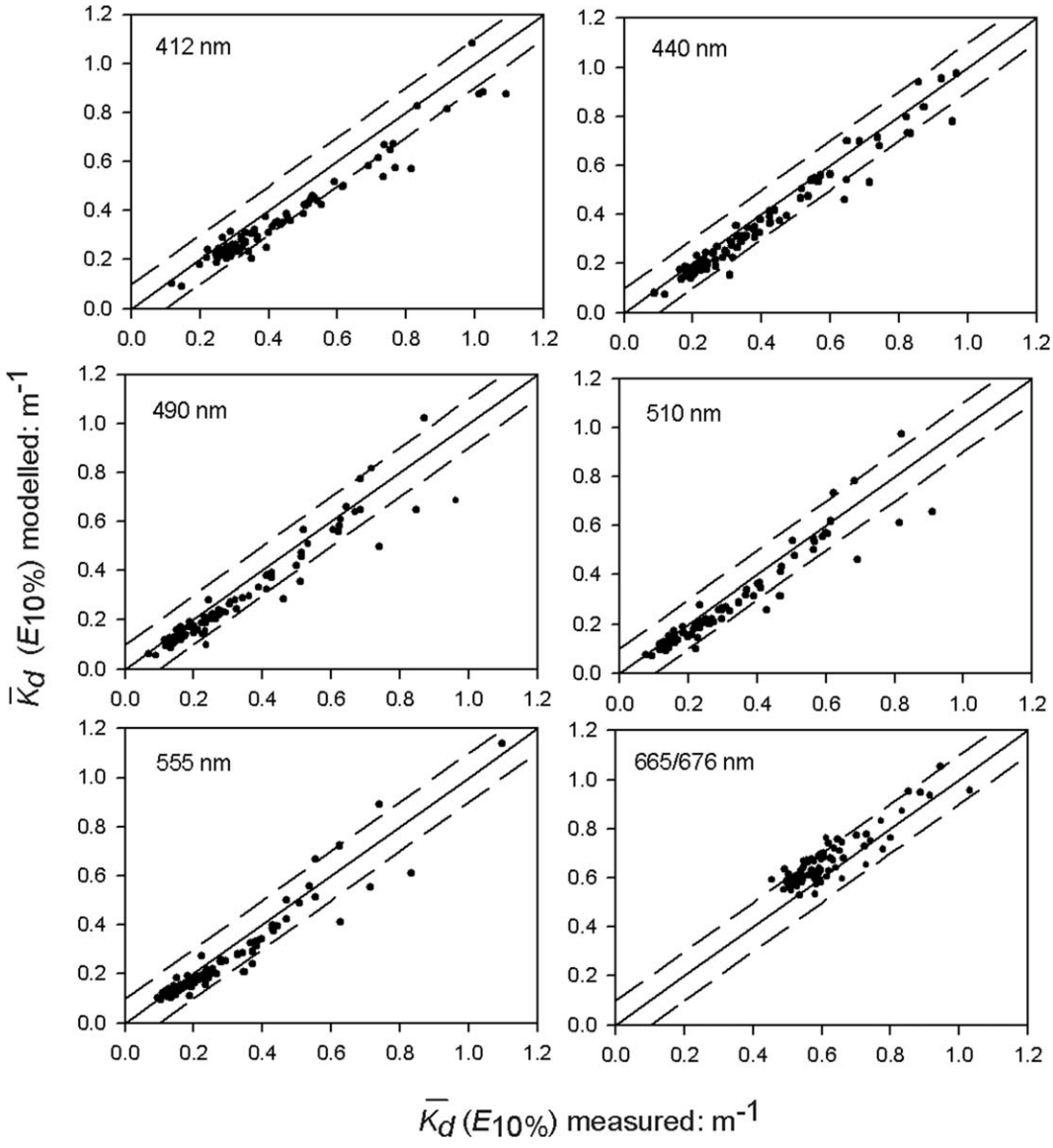

Figure 6. Attenuation coefficients for downward irradiance (for the interval from the surface to the 10% depth for each waveband) calculated using equation (4) plotted against those measured by profiling radiometry. The solid lines indicate 1:1 relationships and dotted lines ± 0.1 m deviations from this relationship.

lower limit and midpoint of the euphotic zone. For the waters studied, SPMR measurements indicate that the reciprocals of these depths bear strong linear relationships to $\overline{K}_d\left(E_{10\%}, 490\text{nm}\right)$. This is illustrated in Figure 7, where the best fit regression lines have coefficients of determination exceeding 0.95, slopes of 0.19 and 0.41, and negligible offsets. Since $\overline{K}_d\left(E_{10\%}, 490\text{nm}\right)$ can be predicted to a fair degree of accuracy using the Lee et al. model (Figure 6), it should be possible to calculate euphotic depths from in situ observations of a(490 nm) and b_b(490 nm). The results of this calculation (Figure 8) indicate that the midpoint of the euphotic zone (10% surface PAR) can be predicted using a power law of the form

$$z_{10\%}, \text{PAR} = 2.44\overline{K}_d\left(E_{10\%}, \lambda\right)^{-0.78}, \tag{5}$$

with an RMS error of 1.25 m over an observed depth range of 2.5–25 m, while the lower limit (1% surface PAR) can be predicted from

$$z_{1\%}, \text{PAR} = 5.27\overline{K}_d\left(E_{10\%}, \lambda\right)^{-0.77}, \tag{6}$$

with root mean square (RMS) error of 3.6 m over a depth range from 4.5 to 50 m.

4. Discussion

[16] Since no attempt has been made to adjust either the in situ observations or the values of the coefficients employed in equation (4), Figure 6 represents a robust test of the model proposed by *Lee et al.* [2005a]. This model

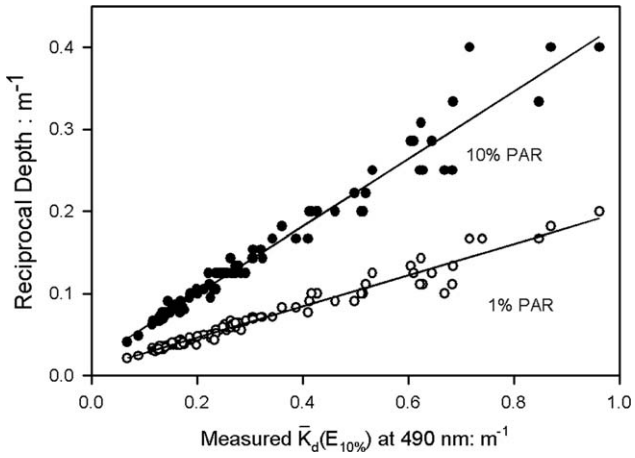

Figure 7. Linear relationships between the downward attenuation coefficient at 490 nm and the reciprocal of the depth at which PAR values fell to 10% and 1% of their surface values for all stations. $\overline{K}_d(E_{10\%}, 490\text{nm})$ and the depths for 1% PAR and 10% PAR were measured by profiling radiometry.

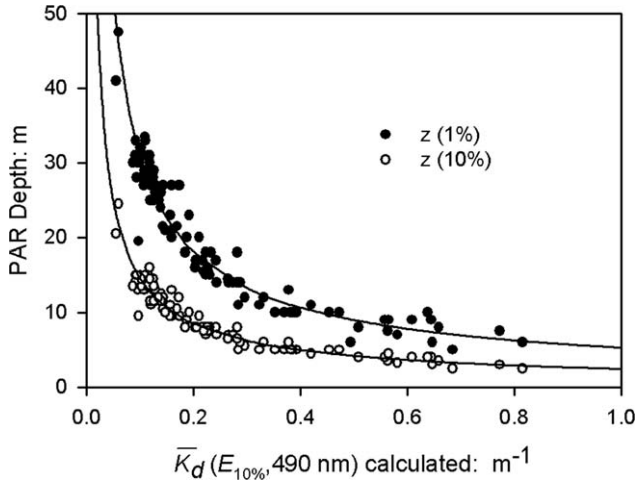

Figure 8. Depths at which in situ PAR measurements reached 10% and 1% of their subsurface values plotted against $\overline{K}_d(E_{10\%}, 490\text{nm})$ calculated using equation (4) with $a(\lambda)$ and $b_b(\lambda)$ values determined in situ for each station. The curves are well described by equations (5) and (6).

works rather effectively as published, and only minor tuning of the coefficients would be required to correct the slight tendency toward underestimation which is evident in these plots. The validation of the Lee et al. model against in situ measurements opens up a wide range of interesting applications. The most obvious is the possibility of calculating $\overline{K}_d(z_1 \rightarrow z_2, \lambda)$ from *IOP* measurements, or from concentrations of phytoplankton, mineral particles and colored dissolved organic matter in waters where the specific optical properties of these constituents are adequately known. Equation (4) also provides a means of estimating the depths from which remote sensing signals originate from *IOP* values, since these depths correspond to $1/\overline{K}_d(\lambda)$ [*Gordon and McCluney*, 1975]. A number of procedures for recovering a (λ) and b_b (λ) from remote sensing reflectance have been proposed [*Lee et al*., 2002; *Liu et al*., 2006; *Doron et al*., 2007] and in waters where these procedures can be validated, equation (4) provides a route to the derivation of $\overline{K}_d(\lambda)$ from remote sensing reflectance signals [*Lee et al*., 2005b]. This may provide a useful alternative to standard empirical algorithms for retrieving K_d (490 nm), which are known to fail in moderately turbid coastal waters [*McKee et al*., 2007; *Wang et al*., 2009].

[17] The relationship demonstrated in Figure 8 between $\overline{K}_d(E_{10\%}, 490\text{nm})$ and the depth of penetration of photosynthetically active radiation was derived for UK west coast waters, but the observations of *Pierson et al*. [2008] in the Baltic Sea suggest that it may have wider geographic applicability. If this is the case, equations (5) and (6) could provide computationally simple means of predicting the effect of changing constituent concentrations on euphotic depths and greatly facilitate calculations of the impact of eutrophication, sediment resuspension, changes in river flow and coastal erosion on light-dependent functions in coastal ecosystems.

[18] **Acknowledgments.** We thank an anonymous reviewer for a useful suggestion for handling the mismatch between ac-9 and SPMR far red wavebands. This work was funded by the UK Natural Environment Research Council.

References

Aksnes, D. L., and J. A. Giske (1993), A theoretical model of aquatic visual feeding, *Ecol. Model.*, *67*, 233–250.

Behrenfeld, M. J., and P. G. Falkowski (1997), A consumer's guide to phytoplankton primary productivity models, *Limnol. Oceanogr.*, *42*, 1479–1491.

Cahill, B., O. Schofield, R. Chant, J. Wilkin, E. Hunter, S. Glenn and P. Bissett (2008), Dynamics of turbid buoyant plumes and the feedbacks on near-shore biogeochemistry and physics, *Geophys. Res. Lett.*, *35*, L10605, doi:10.1029/2008GL033595.

Chang, G., A. Barnard, and J. R. V. Zaneveld (2007), Optical closure in a complex coastal environment: Particle effects, *Appl. Opt.*, *46*, 7679–7692.

Doron, M., M. Babin, A. Mangin, and O. Hembise (2007), Estimation of light penetration, and horizontal and vertical visibility in oceanic and coastal waters from surface reflectance, *J. Geophys. Res.*, *112*, C06003, doi:10.1029/2006JC004007.

Gattuso, J. P., B. Gentili, C. M. Duarte, J. A. Kleypas, J. J. Middelburg, and D. Antoine (2006), Light availability in the coastal ocean: Impact on the distribution of benthic photosynthetic organisms and their contribution to primary production, *Biogeosciences*, *3*, 489–513.

Gordon, H. R. (1989), Can the Lambert-Beer law be applied to the diffuse attenuation coefficient of ocean water? *Limnol. Oceanogr.*, *34*, 1389–1409.

Gordon, H. R., and W. R. McCluney (1975), Estimation of the depth of sunlight penetration in the sea from remote sensing, *Appl. Opt.*, *14*, 413–416.

Gordon, H. R., O. B. Brown and M. M. Jacobs (1975), Computed relationships between inherent and apparent optical-properties of a flat homogeneous ocean, *Appl. Opt.*, *14*, 417–427.

Gower, J. F. R., R. Doerffer, and G. A. Borstad (1999), Interpretation of the 685 nm peak in water-leaving radiance spectra in terms of fluorescence, absorption and scattering, and its observation by MERIS, *Int. J. Remote Sens.*, *20*, 1771–1786.

Kirk, J. T. O. (1984), Attenuation of solar radiation in scattering-absorbing waters: A simplified procedure for its calculation, *Appl. Opt.*, *23*, 3737–3739.

Kirk, J. T. O. (1988), Solar heating of water bodies as influenced by their inherent optical-properties, *J. Geophys. Res.*, *93*, 10,897–10,908.

Lee, Z. P., K. L. Carder, and R. A. Arnone (2002), Deriving inherent optical properties from water color: A multiband quasi-analytical algorithm for optically deep waters, *Appl. Opt.*, *41*, 5755–5772.

Lee, Z. P., K. P. Du, and R. Arnone (2005a), A model for the diffuse attenuation coefficient of downwelling irradiance, *J. Geophys. Res.*, *110*, C02016, doi:10.1029/2004JC002275.

Lee, Z. P., M. Darecki, K. L. Carder, C. O. Davis, D. Stramski, and W. J. Rhea (2005b), Diffuse attenuation coefficient of downwelling irradiance: An evaluation of remote sensing methods, *J. Geophys. Res.*, *110*, C02017, doi:10.1029/2004JC002573.

Leymarie, E., D. Doxaran, and M. Babin (2010), Uncertainties associated to measurements of inherent optical properties in natural waters, *Appl. Opt.*, *49*, 5415–5436.

Liu, C. C., R. L. Miller, K. L. Carder, Z. P. Lee, E. J. D'Sa, and J. E. Ivey (2006), Estimating the underwater light field from remote sensing of ocean color, *J. Oceanogr.*, *62*, 235–248.

McKee, D., A. Cunningham, and A. Dudek (2007), Optical water type discrimination and tuning remote sensing band-ratio algorithms: Application to retrieval of chlorophyll and K-d(490) in the Irish and Celtic Seas, *Estuarine Coastal Shelf Sci.*, *73*, 827–834.

Mobley, C. D. (1994), *Light and Water*, Academic, San Diego, Calif.

Morel, A., and L. Prieur (1977), Analysis of variations in ocean colour, *Limnol. Oceanogr.*, *22*, 709–722.

Neil, C., A. Cunningham, and D. McKee (2011), Relationships between suspended mineral concentrations and red-waveband reflectances in moderately turbid shelf seas, *Remote Sens. Environ.*, *115*, 3719–3730.

Pierson, D. C., S. Kratzer, N. Strombeck, and B. Hakansson (2008), Relationship between the attenuation of downwelling irradiance at 490 nm with the attenuation of PAR (400 nm-700 nm) in the Baltic Sea, *Remote Sens. Environ.*, *112*, 668–680.

Pope, R. M., and E. S. Fry (1997), Absorption spectrum (380–700 nm) of pure water. II. Integrating cavity measurements, *Appl. Opt.*, *36*, 8710–8723.

Rochford, P. A., A. B. Kara, A. J. Wallcraft and R. A. Arnone (2001), Importance of solar subsurface heating in ocean general circulation models, *J. Geophys. Res.*, *106*(30), 923–30,938.

Smith, R. C., and B. R. Marshall (1994), Raman scattering and optical properties of pure water, in *Ocean Optics*, edited by R. W. Spinrad, K. L. Carder, and M. J. Perry, Chapter 12, pp. 226–242, Oxford Univ. Press Oxford University Press, New York.

Sullivan, J. M., M. S. Twardowski, J. R. V. Zaneveld, C. M. Moore, A. H. Barnard, P. L. Donaghay, and B. Rhoades (2006), Hyperspectral temperature and salt dependencies of absorption by water and heavy water in the 400–750 nm spectral range, *Appl. Opt.*, *45*, 5294–5309.

Tassan, S., and G. M. Ferrari (2003), Variability of light absorption by aquatic particles in the near infra-red spectral region, *Appl. Opt.*, *42*, 4802–4810.

Tzortziou, M., J. Herman, C. L. Gallegos, P. J. Neale, A. Subramaniam, L. W. Harding, and Z. Ahmad (2006), Bio-optics of the Chesapeake Bay from measurements and radiative transfer closure, *Estuarine Coastal Shelf Sci.*, *68*, 348–362.

Wang, M. H., S. Son, and L. W. Harding (2009), Retrieval of diffuse attenuation coefficient in the Chesapeake Bay and turbid ocean regions for satellite ocean color applications, *J. Geophys. Res.*, *114*, C10011, doi:10.1029/2009JC005286.

Zaneveld, J. R. V. (1989), An asymptotic closure theory for irradiance in the sea and its inversion to obtain the inherent optical properties, *Limnol. Oceanogr.*, *34*, 1442–1452.

Zaneveld, J. R. V., J. C. Kitchen, and H. Pak (1981), The influence of optical water type on the heating rate of a constant depth mixed layer, *J. Geophys. Res.*, *86*, 6426–6428.

Zaneveld, J. R. V., J. C. Kitchen, and C. Moore (1994), The scattering error correction of reflecting-tube absorption meters, Ocean Optics XII, J.S.Jaffe (ed.) SPIE 2258, 44–55.

Zhai, L., C. Tang, T. Platt and S. Sathyendranath (2011), Ocean response to attenuation of visible light by phytoplankton in the Gulf of St. Lawrence. *J. Mar. Syst.*, *88*, 285–297.